Available online at www.sciencedirect.com
SCIENCE DIRECT®
Talanta 65 (2005) 1295–1302
Talanta
www.elsevier.com/locate/talanta

Synchronous fluorescence and UV–vis spectrometric study of the competitive interaction of chlorpromazine hydrochloride and Neutral Red with DNA using chemometrics approaches

Yongnian Ni[a,*], Daiqin Lin[a], Serge Kokot[b]

[a] *Department of Chemistry, Nanchang University, Nanchang, Jiangxi 330047, China*
[b] *Inorganic Materials Research Program, School of Physical and Chemical Sciences, Queensland University of Technology, Brisbane, Qld. 4001, Australia*

Received 18 June 2004; received in revised form 7 September 2004; accepted 8 September 2004
Available online 2 November 2004

Abstract

In this study, we have shown with the use of UV–vis spectrophotometry and the constant wavelength synchronous fluorescence spectroscopy (CW-SFS) techniques that the pharmaceutical drug, chlorpromazine hydrochloride (CPZ), intercalates into the deoxyribonucleic acid (DNA) double helix by partial exchange with the Neutral Red (NR) molecular probe.

We have also demonstrated that with the use of three-way data plots, it is clear that it is important to have well-defined methodology for the selection of the important CW-SFS method parameter, $\Delta\lambda$. Ad hoc selection of this parameter, or even that based on experience, can readily lead to serious errors, which subsequently can be transferred to the interpretation of results. The said three-way plots provide a straightforward diagrammatic method, which improves the selection process of a satisfactory value for $\Delta\lambda$.

Finally, we used PARAFAC modeling to resolve the complex three-way CW-SFS data, which provided simultaneously the concentration information for the three reaction components, NR, CPZ and NR-DNA, for the system at equilibrium. This PARAFAC analysis indicated that the intercalation of the CPZ molecule into the DNA proceeds by exchanging with the NR probe, and can be attributed to two parallel reactions.

Keywords: Synchronous fluorescence; UV–vis spectrophotometry; PARAFAC; DNA; Chlorpromazine hydrochloride; Neutral Red

1. Introduction

It is well known that deoxyribonucleic acid (DNA) plays an important role in living systems [1], and in recent years, there has been a growing interest in the study of small molecules interacting with calf thymus DNA. The focus has been on the reactions of drugs with DNA, and the investigation of new and effective DNA probes [2–4].

Chlorpromazine hydrochloride (CPZ) (Fig. 1) and related phenothiazines of the neuroleptic group, such as promethazine hydrochloride, propionylpromazine and trifluoperazine, have been used predominantly as psychotropic agents in human and veterinary medication for more than 50 years. Chlorpromazine hydrochloride, the most widely sold drug of this group [5,6], is used as: (i) a peripheral vasodilator, (ii) a tranquilizer, e.g. to reduce preoperative anxiety, (iii) a postoperative anti-emetic, and (iv) a medicine for hiccups, as well as (v) in cancer therapy, and (vi) for control of psychoses [7] such as schizophrenia.

In general, in an organism, the pharmacodynamic mechanism of drugs is always connected with a drug-binding process, which commonly involves the interaction of small amount of a drug with large biomolecules. The biological activity of CPZ also results from its binding interaction with DNA [8,9]. Consequently, binding studies of drugs with DNA

* Corresponding author. Tel.: +86 7918304414; fax: +86 7918305826.
E-mail address: ynni@ncu.edu.cn (Y. Ni).

0039-9140/$ – see front matter © 2004 Elsevier B.V. All rights reserved.
doi:10.1016/j.talanta.2004.09.008

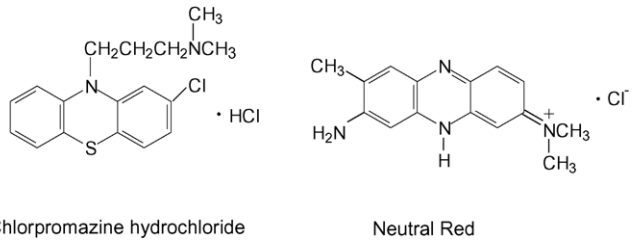

Fig. 1. Structures of chlorpromazine hydrochloride (CPZ) and Neutral Red (NR).

are useful for the understanding of the reaction mechanism as well as for providing guidance for the application and design of new drugs.

Many small molecules are already proven sensitive probes of the DNA structure [10]. Recently, Neutral Red (NR) (Fig. 1) was used as a probe to investigate interactions with calf thymus DNA with the use of spectrophotometry [11] and differential pulse voltammetry [12]. The interaction of NR with DNA involves a two-step mechanism. If the molar ratio of NR to DNA is higher than 1.33, the binding process is characterized by a binding constant of about 10^6 with the binding number close to 1. With lower molar ratios of the interacting components, both the binding number and the constant are lower as well. If there is a large excess of the double-stranded DNA in the interacting system, the binding constant can reach values down to about 10^4 [11]. Also, it has been shown that the binding mode of NR molecules changes from one involving intercalation into the DNA base pairs to one with aggregation along the DNA double helix. Orientation of the NR chromophore in the DNA double helix also changes with temperature [12]. Compared with the classical DNA probes, such as ethidium bromide (EB) [13], Acridine Orange [14], Oxazide Yellow homodimers [15], Nile Blue [16], diphenylamine Blue [17] and indole [18], NR offers lower toxicity, higher stability and convenience. It reacts quickly and is relatively inexpensive [19].

The binding properties of drugs with biological molecules have been investigated with the use of UV spectrophotometry [20], X-ray diffraction [21], voltammetry [22], fluorescence spectroscopy [23] and circular dichroism spectroscopy [24]. With the development of computerized image-processing techniques, high-order analytical instruments and chemometrics algorithms, it is possible to describe objects using multivariate images, and obtain and resolve multi-dimensional data from complex systems. Xie et al. [25,26] investigated the competitive interaction of adriamycin and fluorescence probe EB with DNA, as well as the antitumor drug, daunorubicin, and EB with DNA, by resolving trilinear normal fluorescence data by applying the PARAFAC method. Satisfactory results were obtained. However, the information contained in a conventional excitation-emission matrix (EEM) is insufficient for analysis of a complex system, because there are generally complicated spectral and serious light scattering interferences. In such cases, the synchronous mode of the technique can be applied to eliminate these interferences and increase the resolution capability [27].

In this work, we apply UV–vis spectrophtometry and constant wavelength synchronous fluorescence spectroscopy (CW-SFS) to investigate the interaction of the pharmaceutical drug, CPZ, and DNA with the aid of NR as a molecular probe.

In the case of CW-SFS, a constant wavelength difference, $\Delta\lambda$, must be maintained between the excitation and emission wavelengths. In conventional practice of this technique, it is often difficult to decide the value of this parameter. We investigate the application of three-way modeling with the aim of extracting the preferred value of $\Delta\lambda$, and use this value to obtain the fluorescence results, which provide the necessary information for the interpretation of the interaction of CPZ with DNA.

In addition, we also explore the reaction system consisting of NR, CPZ and NR-DNA complex at equilibrium at pH 7.4 with the use PARAFAC modeling.

2. Theory

2.1. Three-way synchronous fluorescence spectroscopy

Synchronous fluorescence spectroscopy (SFS) was described by Lloyd in 1971 [28,29] and was further developed with the aid of the Vo-Dinh theory [30]. This technique involves the scanning of both the excitation (Ex) and emission (Em) spectra. SFS has become a particularly active field [31,32] because of its apparent advantages, e.g., spectra are simple; there is an improvement in selectivity, and an improvement in spectral resolution because of the generally narrow spectral peaks. There is also a decrease in the interference due to light scattering. There are three variants of SFS [33]: (i) constant wavelength difference (CW), (ii) constant energy difference and (iii) variable-angle or variable-offset techniques, depending on the scanning mode for the spectra. CW-SFS (or simply SFS) is the basic method, and is widely used. It maintains a constant wavelength difference ($\Delta\lambda$) between the excitation and the emission monochromators during the scan.

For CW-SFS, the fluorescence intensity can be expressed as

$$F = klc\,\mathrm{Ex}(\lambda_{\mathrm{Em}} - \Delta\lambda)\mathrm{Em}(\lambda_{\mathrm{Em}}) \quad (1)$$

or

$$F = klc\,\mathrm{Ex}(\lambda_{\mathrm{Ex}})\mathrm{Em}(\lambda_{\mathrm{Ex}} + \Delta\lambda) \quad (2)$$

where $\Delta\lambda = \lambda_{\mathrm{Em}} - \lambda_{\mathrm{Ex}} =$ constant, c is the concentration of analyte, l the path length and k an experimental constant. For a given set of experimental conditions, fluorescence intensity (F) is proportional to the concentration (c) of the analyte.

In this study, three-dimensional plots of synchronous spectra (F versus Ex wavelength and $\Delta\lambda$) were obtained, and then the chemometrics method, PARAFAC, was applied to decompose this three-way data array.

2.2. PARAFAC algorithm

Parallel factor analysis (PARAFAC) is a chemometrics decomposition method, and is a generalization of principal component analysis (PCA) to higher-order arrays [34,35]. However, some of the characteristics of the method are quite different from the common two-way cases. For bilinear methods, there is the well-known problem of rotational freedom, in that the loading vectors obtained from spectral bilinear decomposition can only reflect the pure spectra of analytes measured, but it is not possible to actually find the pure spectra without additional external information. This is not the case for PARAFAC, and an advantage of the PARAFAC model is the resulting unique solution. If the multivariate data are indeed trilinear with an acceptable signal-to-noise ratio, and the appropriate number of components is selected for the model, the true underlying spectra will be found, and the concentrations of analytes can be estimated with the aid of the loadings of the sample profile.

PARAFAC is based on the trilinear theory [36]. A graphical representation (Fig. 2) is presented, and includes a three-component PARAFAC model for the three-way data array, $\boldsymbol{X}$, with dimensions $I \times J \times K$, $\boldsymbol{A}_{I\times H}$, $\boldsymbol{B}_{J\times H}$ and $\boldsymbol{C}_{K\times H}$ containing elements a_{ih}, b_{jh} and $c_{kh.}$ These are the three loading matrices of $\boldsymbol{X}$, in which I indicates the number of $\Delta\lambda$ increments in the experimental wavelength range, J is the wavelength number of Ex (or Em), K indicates the number of samples and H is the number of fluorescing species.

The aim is to resolve the three-way array so as to obtain the three loading matrices. The matrix form of the trilinear model can be expressed as follows:

$$x_{ijk} = \sum_{h=1}^{H} a_{ih} b_{jh} c_{kh} + e_{ijk} \tag{3}$$

where e_{ijk} represents residuals of the three-way array, $\boldsymbol{E}$, and its sum of squares is minimized. The PARAFAC model can also be written as

$$\boldsymbol{X} = \sum_{h=1}^{H} \boldsymbol{a}_h \otimes \boldsymbol{b}_h \otimes \boldsymbol{c}_h + \boldsymbol{E} \tag{4}$$

where the symbol $\otimes$ denotes a tensor product, and vectors $\boldsymbol{a}_h$, $\boldsymbol{b}_h$ and $\boldsymbol{c}_h$ are the hth columns of the loading matrices $\boldsymbol{A}_{I\times H}$, $\boldsymbol{B}_{J\times H}$ and $\boldsymbol{C}_{K\times H}$, respectively.

The solution for PARAFAC model can be found by the alternating least-squares (ALS) algorithm [37] by assuming the loadings in two of the modes are known, and then estimating the unknown set of parameters of the last mode. In other words, if estimates of $\boldsymbol{b}$ and $\boldsymbol{c}$ are given, it is now easily seen that $\boldsymbol{a}$ can be determined by the least-squares solution to the model $\boldsymbol{X} = \boldsymbol{a}(\boldsymbol{b} \otimes \boldsymbol{c})$. If the vector $(\boldsymbol{b} \otimes \boldsymbol{c})$ is called $\boldsymbol{Z}$ in case of more than one component, the model defining $\boldsymbol{A}$ is

$$\boldsymbol{X} = \boldsymbol{A}\boldsymbol{Z} \tag{5}$$

The conditional least-squares estimate of $\boldsymbol{A}$ is

$$\boldsymbol{A} = \boldsymbol{X}\boldsymbol{Z}^{\mathrm{T}}(\boldsymbol{Z}\boldsymbol{Z}^{\mathrm{T}})^{-1} \tag{6}$$

A typical iterative procedure is as follows:

- Step 1: Estimate the number of chemical components, H.
- Step 2: Initialize matrices of $\boldsymbol{B}$ and $\boldsymbol{C}$, and estimate $\boldsymbol{A}$ from $\boldsymbol{X}$, $\boldsymbol{B}$ and $\boldsymbol{C}$ by least-squares regression.
- Step 3: Estimate matrices of $\boldsymbol{B}$ and $\boldsymbol{C}$ in the same way as in step (2).
- Step 4: Continue the iteration from (2) until convergence.

The ALS algorithm is similar to the above description, namely initialize $\boldsymbol{B}$ and $\boldsymbol{C}$ and estimate $\boldsymbol{A}$, then similarly estimate $\boldsymbol{B}$, from $\boldsymbol{C}$ and $\boldsymbol{A}$, and do the same for $\boldsymbol{C}$ with the use of $\boldsymbol{A}$ and $\boldsymbol{B}$. Repeat steps (2) and (3) until convergence is achieved. The important difference between PCA and PARAFAC is that in PARAFAC there is no need for orthogonality between the three loading matrices ($\boldsymbol{A}$, $\boldsymbol{B}$ and $\boldsymbol{C}$) to describe the model, and the solution is unique.

3. Experimental

3.1. Apparatus

Molecular absorption spectra were measured on a Shimadzu UV-2501 Spectrophotometer using 1.0 cm quartz cells. Synchronous fluorescence spectra measurements were performed on a Hitachi F-3010 spectrofluorometer equipped with a 150 W xenon lamp, and with the use of a 1.0 cm × 1.0 cm quartz cell. The excitation and emission slits were set at 10 nm. The synchronous flu-

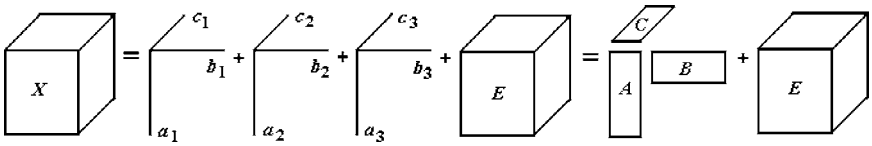

Fig. 2. Graphical representation of a two-component PARAFAC model of the data array $\boldsymbol{X}$.

orescence signal was recorded by scanning both excitation and emission wavelengths simultaneously at a rate of 600 nm min^{-1}.

3.2. Chemical reagents

The stock solution of calf thymus DNA (ct-DNA) (Beitai Biochemical Co., Chinese Academy of Sciences, Beijing) was prepared by dissolving the solid DNA in doubly distilled water and stored at 4 °C. The concentration of the DNA was determined at 260 nm taking the value of molar absorptivity as 6600 l mol^{-1} cm^{-1} [11]. This was carried out after establishing that the absorbance ratio A_{260}/A_{280} was in the range 1.8–1.9 [38]. The solution used in this experiment was not purified further.

Chlorpromazine hydrochloride (Hefeng Co., Shanghai) was in the form of a solution used for clinical injections, and contained 50 mg of CPZ per phial. This solution was diluted with doubly distilled water [39] so as to produce a 7.02×10^{-3} mol l^{-1} stock solution.

A 1.00×10^{-4} mol l^{-1} stock solution of Neutral Red (The Third Reagent Factory, Shanghai) was prepared by directly dissolving its crystals in water, and diluting to the required volume. Subsequently, all solutions were adjusted with the Tris–HCl buffer (Tris–(hydroxy methyl)amino methane–hydrogen chloride) to a pH of 7.4. Other reagents were of analytical-reagent grade, and doubly distilled water was used throughout.

3.3. Procedure

One milliliter of 1.00×10^{-4} mol l^{-1} NR, 2.0 ml of Tris–HCl buffer and the appropriate amount of DNA solution were added to a 10 ml volumetric flask, diluted to 10 ml with doubly distilled water, and mixed thoroughly. This solution was allowed to stand for 5 min, and then spectrophotometric and spectrofluorimetric NR data were collected from solutions of different DNA concentrations.

Different amounts of CPZ were added to a series of 10 ml volumetric flasks containing 1.0 ml of 1.00×10^{-4} mol l^{-1} NR, 0.4 ml of 1.935×10^{-3} mol l^{-1} DNA and 4.0 ml of Tris–HCl buffer. These solutions were diluted to the mark with doubly distilled water. The concentration range of CPZ was 2.34×10^{-5} to 1.64×10^{-4} mol l^{-1}, and the binding reaction was carried out at 25 ± 1 °C. Spectrofluorimetric measurements of seven such samples were carried out over the excitation wavelength range 220–700 nm at 10 nm intervals (total 49 wavelengths), and Δλ was changed in the range 30–120 nm at 10 nm intervals (total number of Δλ increments is 10). Thus, the three-way data, ***X***, to be decomposed has the dimensions of 10 × 49 × 7 corresponding to the *I*, *J* and *K* in Section 2.2, respectively. ***A***, ***B*** and ***C*** loadings matrices are extracted by application of the PARAFAC, and of these ***B*** and ***C*** are the estimated excitation spectra, Ex, and the equilibrium concentrations of the reaction components, respectively.

4. Results and discussion

4.1. Investigation of the binding of NR to DNA

4.1.1. UV–vis spectrophotometry

In general, if a small molecule interacts with DNA, changes in absorbance (hypochromism) and in the position of the band (red shift) should occur. When they do, they indicate that the small molecule has intercalated between DNA base pairs, and is involved in a strong interaction in the molecular stack between the aromatic chromophore and the base pairs. The spectral effects have been rationalized as follows [40–42]: the empty π^*-orbital of the small molecule couples with the π-orbital of the DNA base pairs, which causes an energy decrease, and a decrease of the $\pi \rightarrow \pi^*$ transition energy. Therefore, the absorption of the small molecule should exhibit a red shift. At the same time, the empty π^*-orbital is partially filled by electrons, reducing the transition probability, and this leads to hypochromism.

In our work, UV–vis spectra were recorded from solutions of the NR at fixed concentration mixed with different concentrations of the DNA (Fig. 3). In general, there is a maximum absorption at about 454 nm in the spectrum of an NR solution when DNA is present. It was found that the band absorbance at 454 nm decreased with an observed hypochromicity of 24.7%, and a small red shift (11 nm) was evident with the increasing concentration of DNA. A band developed at approximately 500 nm with increasing DNA concentration, and has been assigned to the NR-DNA complex. It increases in intensity with DNA, and has a bathochromic shift to 540 nm. An isosbestic point is present at 498 nm. These spectral results indicate that NR is an intercalator whose chromophore inserts partially into the base pairs.

4.1.2. Synchronous fluorimetry

The experiments for the selection of an appropriate value of the parameter, Δλ (Section 3.3), for solutions with or without DNA gave the preferred result of 60 nm. The synchronous fluorescence excitation spectrum of NR (Fig. 4) exhibits an

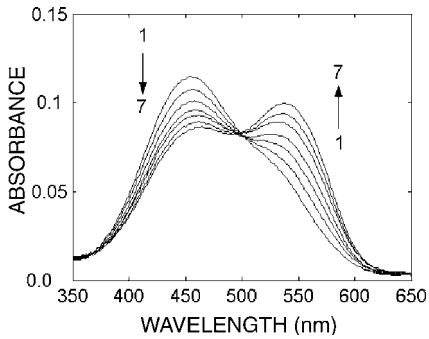

Fig. 3. Adsorption spectra of NR in the presence of DNA with different concentrations: $c_{NR} = 1.00 \times 10^{-5}$ mol l^{-1} and c_{DNA} = 0, 0.645, 1.29, 1.94, 2.58, 3.23 and 3.87×10^{-5} mol l^{-1}, corresponding to the curves from 1 to 7, respectively.

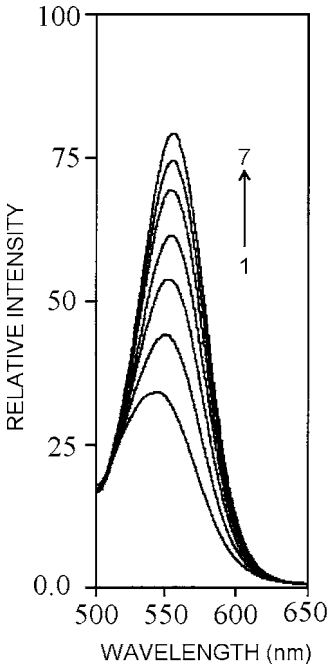

Fig. 4. Synchronous fluorescence spectra of NR in the presence of DNA with different concentrations: $\Delta\lambda = 60$ nm, $c_{NR} = 1.00 \times 10^{-5}$ mol l^{-1} and $c_{DNA} = 0$, 0.645, 1.29, 1.94, 2.58, 3.23 and 3.87 $\times 10^{-5}$ mol l^{-1}, corresponding to the curves from 1 to 7, respectively.

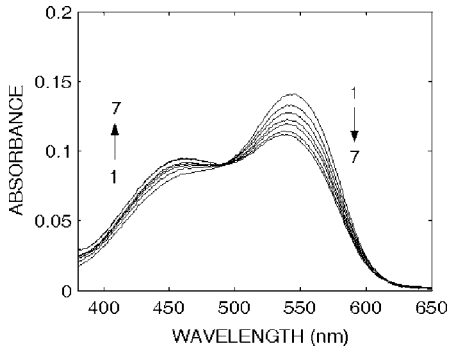

Fig. 5. Effect of CPZ on absorption spectra of NR-DNA: $c_{DNA} = 7.74 \times 10^{-5}$ mol l^{-1}, $c_{NR} = 1.00 \times 10^{-5}$ mol l^{-1}, and $c_{CPZ} = 2.34$, 4.68, 7.02, 9.36, 11.7, 14.0 and 16. 4×10^{-5} mol l^{-1}, corresponding to the curves from 1 to 7, respectively.

excitation maximum at 545 nm in the wavelength range from 500 to 650 nm. Generally, the fluorescence band intensity attributed to NR is relatively weak, but in common with UV–vis spectra described above, the fluorescence intensity at 545 nm increased and shifted to 560 nm with the increasing concentration of DNA. Such spectral effects are similar to those observed in the interaction of ethidium bromide (EB) and DNA [41]. This molecule is well known as a typical intercalator, and it has a weak fluorescence, which in the presence of DNA is significantly enhanced. This is attributed to strong intercalation of EB between the adjacent DNA base pairs. Thus, on this basis, the enhancement of fluorescence intensity of the NR excitation band with concentration of DNA indicates that NR intercalates into the DNA double helix. This observation supports the results obtained from the UV–vis spectra.

4.2. Effect of CPZ on the absorption spectra of NR-DNA

As shown in Fig. 5, with increasing concentration of CPZ, the maximum absorption at 540 nm of the NR-DNA spectrum decreases but a slight intensity increase is observed in the developing band at 454 nm. When this observation is compared to the behaviour of the free NR absorption band at 454 nm (Fig. 3) in the presence of increasing concentration of DNA, it is noted that its intensity increases.

The observed changes in intensity and position of the bands with increasing amounts of CPZ added to the NR-DNA complex solution suggest that some of the NR molecules, which were intercalated into the DNA base pairs, were exchanged by CPZ. This is consistent with the view that planarity of a molecule is one of the necessary conditions for efficient intercalation into the double helix [43]. An aromatic ring stacking between nucleobase pairs is regarded as a major driving force for binding of an intercalator into the double helix. Since the CPZ molecule contains a planar aromatic ring (Fig. 1), which can stack between DNA bases, CPZ should be able to intercalate into the double helix. Thus, considering the above results, it is evident that with the use of NR as an indicator, and UV–vis spectrophotometry to probe the interaction between CPZ and DNA under neutral pH conditions, the drug, CPZ, binds to DNA by intercalating between the base pairs.

4.3. Three-way synchronous fluorescence data of NR, CPZ and NR-DNA

In most synchronous spectrofluorimetric studies of chemical systems, the selection of $\Delta\lambda$ is very important with the classical two-dimensional SF. The influence of $\Delta\lambda$ can be substantial on the shape, location and signal intensity of a fluorescence peak, as well as on interferences attributed to light scattering. In general, the selection of the value for $\Delta\lambda$ is based on experience. In this work, in order to get the best value of $\Delta\lambda$ and to investigate thoroughly the chemical system, three-way SF data were sampled and studied. The three-way data plots for NR-DNA, NR and CPZ (Figs. 6–8) show that the preferred values of $\Delta\lambda$ for the three systems are quite different. In Fig. 6, it can be clearly seen that the fluorescence intensity of NR-DNA varied with the different values of $\Delta\lambda$, and with the optimal value for NR-DNA being 60 nm (see arrow). On the other hand, the excitation wavelength, Ex, shows a blue shift from 580 to 500 nm with increasing value of $\Delta\lambda$ from 20 to 110 nm. Similarly, the best value of $\Delta\lambda$ for NR (130 nm) can be found from Fig. 7, and Ex wavelength changed from 560 to 430 nm with increasing value of $\Delta\lambda$ from 30 to 210 nm. The behaviour of CPZ (Fig. 8) is quite different from the other two cases. The fluo-

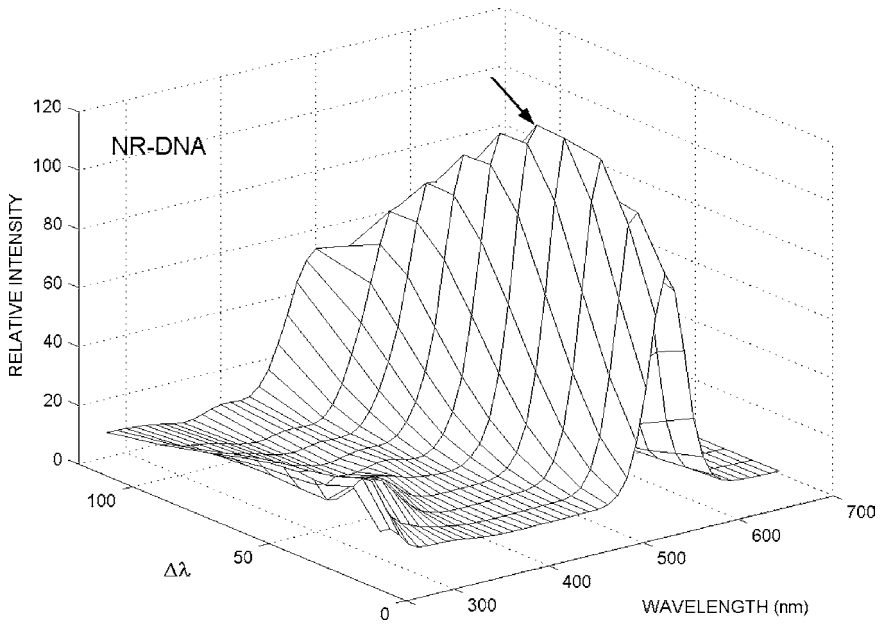

Fig. 6. Synchronous fluorescent spectra of NR-DNA.

rescence peak varies significantly with different $\Delta\lambda$ values. The most intense peak of CPZ appears at a $\Delta\lambda$ value of about 140 nm. Thus, the advantage of the three-way approach now becomes apparent. With the conventional two-way SF approach where $\Delta\lambda$ is fixed at one value, errors will clearly arise in any simultaneous investigation of the NR, CPZ and NR-DNA complex system. These errors may be avoided with the use of the three-way SF methodology for the selection of $\Delta\lambda$ values.

4.4. Decomposition of the three-way synchronous fluorescence spectrum by PARAFAC

The three-component PARAFAC algorithm was applied to investigate the competitive binding interactions of the complex system consisting of CPZ, NR and DNA, and to understand their states at equilibrium.

NR was adopted as the fluorescence probe to study the interaction of the pharmaceutical drug, CPZ, with DNA, and

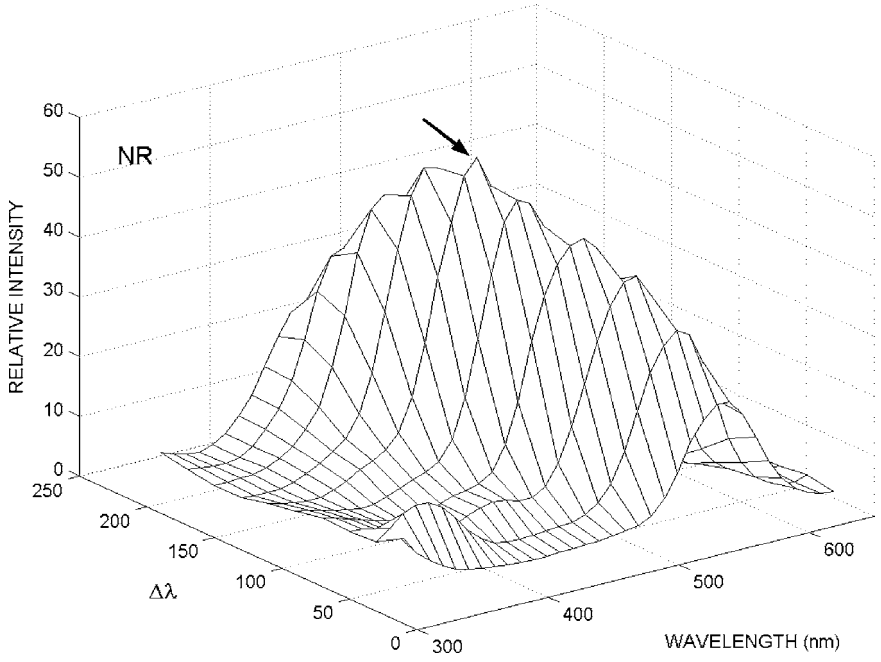

Fig. 7. Synchronous fluorescent spectra of NR.

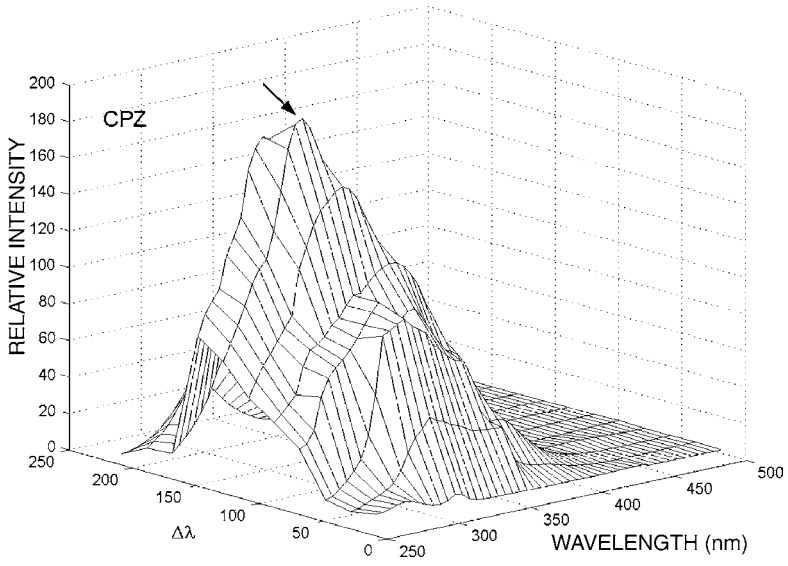

Fig. 8. Synchronous fluorescent spectra of CPZ.

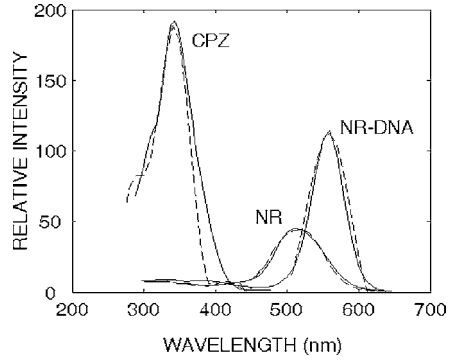

Fig. 9. Comparison of the true excitation spectra, Ex, for CPZ, NR and NR-DNA with those obtained from PARAFAC analysis. Dashed line: resolved spectra from PARAFAC; solid line: recorded true spectra.

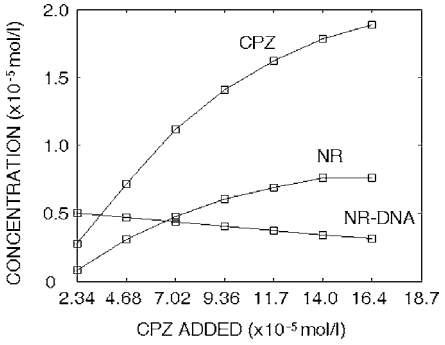

Fig. 10. Equilibrium concentrations of CPZ, NR and NR-DNA resolved by the PARAFAC model. CPZ was present at CPZ at different concentrations.

all solutions were prepared with concentrations as described in Section 3.3.

Excitation loadings (matrix ***B***) obtained from NR-DNA, NR and CPZ solutions with the use of PARAFAC algorithm modeling (dashed lines, Fig. 9), indicate that the estimated excitation spectra are quite similar to the measured ones (solid lines). This suggests that the results are unique, reliable and the correct number of factors has been chosen. Generally, when applying the PARAFAC method, one or two extra factors than the real number of chemical components are chosen to account for the influence of interferents [44]. In this study, only three factors were selected because the system is free of any interferents. Furthermore, the extracted loadings from the spectra were used to estimate the state of equilibrium. The relative equilibrium concentrations of NR-DNA, NR and CPZ resolved by the PARAFAC model (the rows in the loading matrix ***C***, Fig. 10) can be considered to reflect the real reacting fluorescing species studied in the system because PARAFAC only gives unique solutions.

From Fig. 10, it can be seen that the concentration of the complex NR-DNA decreased and the one for free NR increased gradually with increasing concentration of the added CPZ. The replacement of NR in the NR-DNA complex by free CPZ can be visualized clearly, and the results indicated that CPZ intercalates into the same base sites of DNA releasing the bound NR. The binding reactions are a pair of parallel competitive reactions, and the interaction of CPZ with DNA is also assumed to belong to the intercalation model, with the CPZ molecules intercalating between the base pairs of double-stranded DNA.

5. Conclusion

In this study, we have shown that with the use of UV–vis spectrophotometry and the CW-SFS techniques the pharmaceutical drug, CPZ, intercalates into the DNA double helix by partial exchange with the NR molecular probe in the presence of the Tris–HCl buffer at pH 7.4.

We have also demonstrated with the use of the three-way data plots, that it is important to have well-defined methodology for the selection of the important CW-SFS method parameter, $\Delta\lambda$. Ad hoc selection, or even that based on experience, can readily lead to serious errors, which subsequently can be transferred to the interpretation of results. The said three-way plots provide a straightforward diagrammatic method, which improves the selection process of $\Delta\lambda$ values.

Finally, we used PARAFAC modeling to resolve the complex three-way CW-SFS data, which provided simultaneously the concentration information for the three reaction components, NR, CPZ and NR-DNA, in the system at equilibrium. This indicated that the intercalation of the CPZ molecule into the DNA proceeds by exchanging with the NR probe, and can be thought of as progressing by two parallel reactions.

Acknowledgements

The authors gratefully acknowledge the financial support of this study by the National Science Foundation of China (No. 20365002), the State Key Laboratories of Electroanalytical Chemistry (No. SKLEAC2004-3) and Chemo/Biosensing and Chemometrics of Hunan University (No. 2002-18), the Jiangxi Province Natural Science Foundation (No. 0320014), the Key Laboratory of Food Sciences of MOE and the Analytical and Test Centre of Nanchang University.

References

[1] P. Yang, F. Gao, The Theory of Bioinorganic Chemistry, Chinese Science Press, Beijing, 2002, p. 29.
[2] D.H. Tjahjono, T. Akutsu, N. Yoshioka, H. Inoue, Biochim. Biophys. Acta: Gen. 1472 (1999) 333.
[3] T. Uno, K. Hamasaki, M. Tanigawa, S. Shimabayashi, Inorg. Chem. 36 (1999) 1676.
[4] J. Liu, G.A. Luo, Y.M. Wang, H.W. Sun, Acta Pharmacol. Sin. 36 (2001) 74.
[5] D. Li, Pharmacology, The Chinese People's Healthy Press, Beijing, 1999, p. 123.
[6] F. Lopez-Munoz, C. Alamo, G. Rubio, E. Cuenca, Prog. Neuro-Psychol. Biol. Psychol. 28 (2004) 205.
[7] R.J. Baldessarino, in: L.S. Goodman, A. Gilman (Eds.), The Pharmacological Basis of Therapeutics, 6th ed., McMillan, New York, 1980, p. 391.
[8] J. Wang, G. Rivas, X. Cai, H. Shiraishi, P.A.M. Farias, N. Dontha, D. Luo, Anal. Chim. Acta 332 (1996) 139.
[9] B.S. Fujimoto, J.B. Clendenning, J.J. Delrow, P.J. Heath, M. Schurr, J. Phys. Chem. 98 (1994) 6633.
[10] L.S. Ling, Z.K. He, Y.E. Zeng, Chin. J. Anal. Chem. 29 (2001) 721.
[11] C.Z. Huang, Y.F. Li, P. Feng, Talanta 55 (2001) 321.
[12] Z.X. Wang, Z.L. Zhang, D.J. Liu, S.J. Dong, Spectrochim. Acta A 59 (2003) 949.
[13] L. Vergani, G. Mascetti, P. Gavazzo, C. Nicolini, Thermochim. Acta 294 (1997) 193.
[14] Y. Cao, X.W. He, Z. Cao, L. Peng, Talanta 49 (1999) 377.
[15] H.S. Rye, J.M. Dabora, M.A. Quesada, R.A. Mathies, A.N. Glazer, Anal. Biochem. 208 (1993) 144.
[16] Q.Y. Chen, D.H. Li, Y. Zhao, H.H. Yang, Q.Z. Zhu, J.G. Xu, Analyst 124 (1999) 901.
[17] M.V. Lancker, L.C. Gheyssens, Anal. Lett. 19 (1986) 615.
[18] R.W. Hubbard, W.T. Matthew, D.W. Moulton, Anal. Biochem. 173 (1972) 46.
[19] Y. Cao, X.W. He, G.Z. Zhang, Chem. J. Chin. Univ. 20 (1999) 709.
[20] G. Viola, L. Latterini, D. Vedaldi, G.G. Aloisi, F. Dall'Acqua, N. Gabellini, F. Elisei, A. Barbafina, Chem. Res. Toxicol. 16 (2003) 644.
[21] P. Karmadar, U.B. Dasgupta, R.K. Poddar, Curr. Sci. 68 (1995) 537.
[22] J. Zhong, Z.M. Qi, H. Dai, C.H. Fan, G.X. Li, N. Matsuda, Anal. Sci. 19 (2003) 653.
[23] W.J. Jin, W.H. Liu, X. Yang, Y.M. Zhang, G.L. Shen, R.Q. Yu, Microchem. J. 61 (1999) 115.
[24] M.P. Singh, T. Joseph, S. Kumar, Y. Bathini, J.W. Lown, Chem. Res. Toxicol. 5 (1992) 597.
[25] H.P. Xie, X. Chu, J.H. Jiang, H. Cui, G.L. Shen, R.Q. Yu, Spectrochim. Acta A 59 (2003) 743.
[26] H.P. Xie, J.H. Jiang, X. Chu, H. Cui, G.L. Shen, R.Q. Yu, Anal. Bioanal. Chem. 373 (2002) 159.
[27] X.J. Yang, J. Chou, G.Q. Sun, H. Yang, T.H. Lu, Microchem. J. 60 (1998) 210.
[28] J.B.F. Lloyd, Nature 231 (1971) 64.
[29] J.B.F. Lloyd, Forens. Sci. Soc. 11 (1971) 83.
[30] T. Vo-Dinh, Anal. Chim. Acta 185 (1986) 1.
[31] H. Ghatak, S.K. Mukhopadhyay, H. Biswas, S. Sen, T.K. Jana, Indian J. Mar. Sci. 31 (2002) 136.
[32] C.Q. Jiang, J.X. He, J. Pharm. Biomed. Anal. 29 (2002) 737.
[33] E.L. Wehry, Modern Fluorescence Spectroscopy, vol. 4, Plenum Press, New York, 1981, p. 252.
[34] R.A. Harshman, S.A. Berenbaum, in: D.H. Eichorn, J.A. Clausen, N. Haan, M.P. Honzik, P.H. Mussen (Eds.), Present and Past in Middle Life, Academic Press, New York, 1981, p. 435.
[35] D.S. Burdick, Chemom. Intell. Lab. Syst. 28 (1995) 229.
[36] R.A. Harshman, M.E. Lundy, Comput. Stat. Data Anal. 18 (1994) 39.
[37] R. Bro, Chemom. Intell. Lab. Syst. 38 (1997) 149.
[38] Z.Y. Chen, J. Liu, D. Luo, Biochemistry Experiments, Chinese University of Science and Technology Press, Hefei, 1994, p. 111.
[39] Chinese Pharmacopoeia Committee, Pharmacopoeia, Chemical Industry Press, Beijing, 1995.
[40] E.C. Long, J.K. Barton, Acc. Chem. Res. 23 (1990) 273.
[41] J. Liu, T.B. Lu, H. Li, Q.L. Zhang, L.N. Ji, Transit. Metal Chem. 27 (2002) 686.
[42] S.A. Tysoe, R.J. Morgan, A.D. Baker, T.C. Strekas, Phys. Chem. 97 (1993) 1707.
[43] L.S. Lerman, Mol. Biol. 3 (1961) 18.
[44] R. Bro, Chemom. Intell. Lab. Syst. 46 (1999) 133.